GEOLOGY | THE GEOLOGICAL SOCIETY OF AMERICA®

https://doi.org/10.1130/G51849.1

Manuscript received 19 December 2023
Revised manuscript received 9 February 2024
Manuscript accepted 18 February 2024

Published online 22 March 2024

© 2024 The Authors. Gold Open Access: This paper is published under the terms of the CC-BY license.

Ice? Salt? Pressure? Sediment deformation structures as evidence of late-stage shallow groundwater in Gale crater, Mars

Steven G. Banham[1,*], Amelie L. Roberts[1], Sanjeev Gupta[1], Joel M. Davis[1], Lucy M. Thompson[2], David M. Rubin[3], Gerhard Paar[4], Kirsten L. Siebach[5], William E. Dietrich[6], Abigail A. Fraeman[7], and Ashwin R. Vasavada[7]

[1]Department of Earth Science & Engineering, Imperial College London, London SW7 2BP, UK
[2]Planetary & Space Science Centre, University of New Brunswick, Fredericton, New Brunswick E3B 5A3, Canada
[3]Department of Earth & Planetary Sciences, University of California, Santa Cruz, California 95064, USA
[4]Joanneum Research Institute for Information and Communication Technologies, 8010 Graz, Austria
[5]Department of Earth & Planetary Sciences, Rice University, Houston, Texas 77251, USA
[6]Department of Earth & Planetary Science, University of California, Berkeley, California 94720, USA
[7]Jet Propulsion Laboratory, California Institute of Technology, Pasadena, California 91011, USA

ABSTRACT

Persistence of near-surface water during the late evolution of Gale crater, Mars, would have been fundamental for maintaining a habitable environment. Sedimentation in aqueous conditions is evident during the early stages of crater infilling, where accumulation of lower Mount Sharp group strata is characterized by fluviolacustrine sedimentary rocks. The basal unit of the Siccar Point group—the Stimson formation—which unconformably overlies the Mount Sharp group and represents conditions postdating the exhumation of Aeolis Mons, is characterized by accumulation of aeolian strata under arid conditions. Water was largely absent near the surface during its deposition. At the Feòrachas outcrop, discovery of soft sediment deformation structures in aeolian Stimson strata challenges the notion that Gale crater was devoid of water during its later depositional phase. We identified deformed wind-rippled and vertically laminated sandstones, hosted within erosion-resistant ridges forming boxwork patterns. Broadly, these structures are diagnostic of water (as liquid or as ice) in the shallow subsurface. Comparison with Earth analogues suggests formation by subsurface fluid escape, freeze-thaw processes, or evaporite deformation. Regardless of the mechanism, these structures signify the presence of water at or near the surface much later than previously documented and may extend the habitability window in Gale crater.

INTRODUCTION

During the initial infilling of Gale crater, water was a prime agent for sediment transport and contributed toward creating habitable conditions. Exploration of the central sediment mound within Gale crater—Aeolis Mons, informally Mount Sharp—using the Mars Science Laboratory rover *Curiosity* (herein, *Curiosity*), revealed that the oldest crater-filling strata—the lower part of the Mount Sharp group—largely record sediment accumulation in fluviolacustrine environments (Grotzinger et al., 2015; Gwizd et al., 2022). Higher in the Mount Sharp group, fluviolacustrine strata are supplanted by increasing aeolian strata, interpreted as progressive aridification of surface conditions. This gradational boundary represents a major climate transition between early humid and later arid conditions within Gale crater, if not more extensively on Mars (Bibring et al., 2006; Milliken et al., 2010). The Mount Sharp group has been the focus for the investigation of habitability by *Curiosity*.

The Mount Sharp group is incised by a major erosional surface, the Siccar Point unconformity, which mirrors the shape of present-day Aeolis Mons (Watkins et al., 2022). Superimposed on this unconformity, there is a regionally extensive draping unit, defined from prelanding orbital observations as the mound skirting unit (Anderson and Bell, 2010). Where traversed by the rover, it is defined as the Stimson formation, forming the base of the Siccar Point group. The Stimson formation represents the preserved expression of a dry dune field (Banham et al., 2018), and it outcrops in several areas: Emerson plateau, Naukluft plateau, Murray buttes, and the Greenheugh pediment. These Stimson outcrops record accumulation of sediment in a surface environment devoid of water, within a regionally arid climate (Banham et al., 2018, 2022), suggesting diminished habitability (Westall et al., 2015; Ehlmann et al., 2016).

On the east side of the Greenheugh pediment (Fig. 1) at the base of the Stimson formation, deformation structures were observed in the aeolian cross-strata. Here, cross-laminations are contorted, deformed, or crosscut by vertical laminations within now well-cemented, erosion-resistant sandstone ridges. These structures are interpreted as evidence of shallow groundwater, which could have provided a subsurface environment that could have reasonably extended the habitability window within Gale crater.

BACKGROUND

Evidence for diagenesis and aqueous processes is pervasive throughout Mount Sharp's stratigraphy. Filled fractures are abundant within the Murray formation (Nachon et al., 2014; Kronyak et al., 2019), forming subvertical, calcium sulfate–filled veins generated by hydraulic fracturing (Cosgrove et al., 2022) and mobilization of primary salt from within the stratigraphy. Cylindrical injection pipes are

Steven G. Banham https://orcid.org/0000-0003-1206-1639
*sbanham@ic.ac.uk

CITATION: Banham, S.G., et al., 2024, Ice? Salt? Pressure? Sediment deformation structures as evidence of late-stage shallow groundwater in Gale crater, Mars: Geology, v. 52, p. 492–496, https://doi.org/10.1130/G51849.1

Downloaded from http://pubs.geoscienceworld.org/gsa/geology/article-pdf/52/7/492/6508686/g51849.1.pdf
by guest

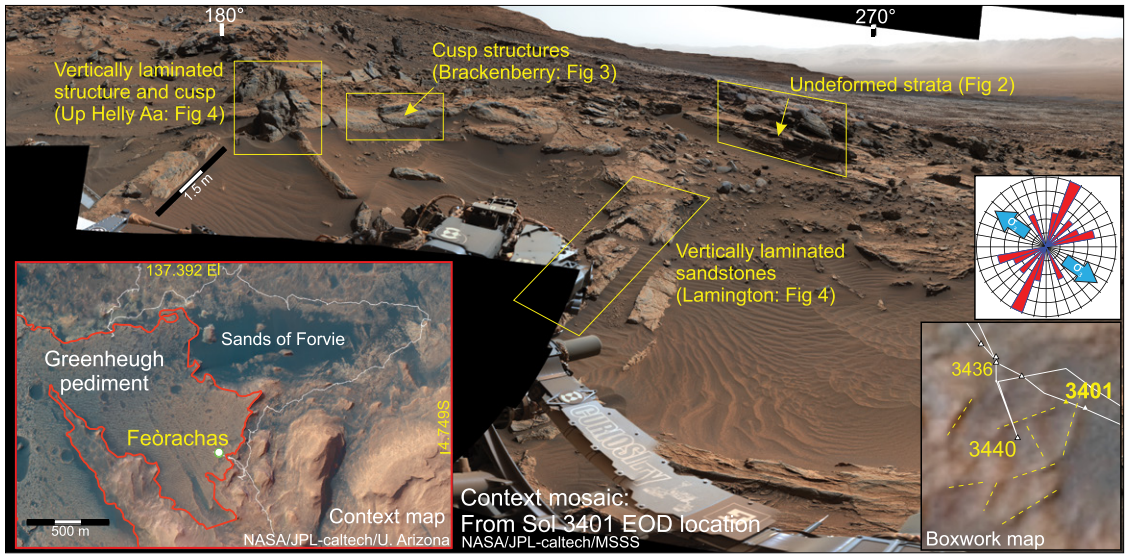


Figure 1. Overview of Feòrachas structure, depicting geometries of lineaments and locations of key observations. Context map shows rover traverse (white line). Boxwork map shows orientation of ridges. Rose diagram depicts orientation of those ridges (resultant 215°, *n* = 10). Credit: NASA/JPL-Caltech/MSSS.

present in the Mount Sharp group, which were triggered by impacts, hydraulic overpressure, or seismic shock (Rubin et al., 2017). Cylindrical pipes indicate no differential stress or that sediment was unconsolidated at time of injection (Cosgrove, 1995). Diagenetic concretions are ubiquitous across the base of the Stimson formation (Banham et al., 2018, 2021, 2022). Silica-enriched, fracture-associated alteration halos have been observed at Emerson and Naukluft plateaus, indicating late-stage high-temperature (>80 °C) groundwater circulation (Yen et al., 2017). Finally, deformation structures identified in the basal Stimson formation on the eastern Greenheugh pediment (Dietrich et al., 2022) are linked to the nodule-rich basal facies.

STUDY LOCATION: GREENHEUGH PEDIMENT

On the east margin of the Greenheugh pediment (mission Sols 3401–3444; Fig. 1, context. See Supplemental Material[1] for additional images), series of prominent rectilinear sandstone ridges were identified within the Stimson formation using *Curiosity*'s Mastcam cameras (Malin et al., 2017). Informally named the Feòrachas structure (also described as a "boxwork" structure; Fig. 1), these erosion-resistant sandstone ridges are 25–50 cm wide, 2.5–5 m in length, and a few decimeters tall. Some sections have a prominence of 1 m above the surrounding bedrock and regolith. The long axis of the boxworks are typically oriented NNE-SSW or ENE-WSW (Fig. 1, rose diagram: vector mean = 215°). Sandstone enclosed within the boxwork structure is undeformed. Internally, ridges are well cemented and preserve sedimentary structures corresponding to either primary depositional processes or penecontemporaneous deformation. Four key sublocalities within the Feòrachas outcrop are used to illustrate the main sedimentary structures: undeformed aeolian strata, liquefaction cusps (Brackenberry), and vertically laminated sandstone dikes (Up Helly Aa and Lamington; Fig. 1).

[1]Supplemental Material. Slide pack of high-quality images used as part of this study and additional data. Please visit https://doi.org/10.1130/GEOL.S.25263151 to access the supplemental material; contact editing@geosociety.org with any questions.

DESCRIPTION OF SEDIMENTARY STRUCTURES

Undeformed Aeolian Strata

Undeformed aeolian cross-strata are exposed adjacent to Feòrachas (Fig. 2) and share common facies and architectural attributes with the Stimson formation at the north edge of the Greenheugh pediment (Banham et al., 2022) and elsewhere along the traverse (Banham et al., 2021; Bedford et al., 2020). Here, the Stimson formation is composed of compound cross-beds (10–50 cm thick), containing uniform-thickness, laterally persistent, wind-ripple

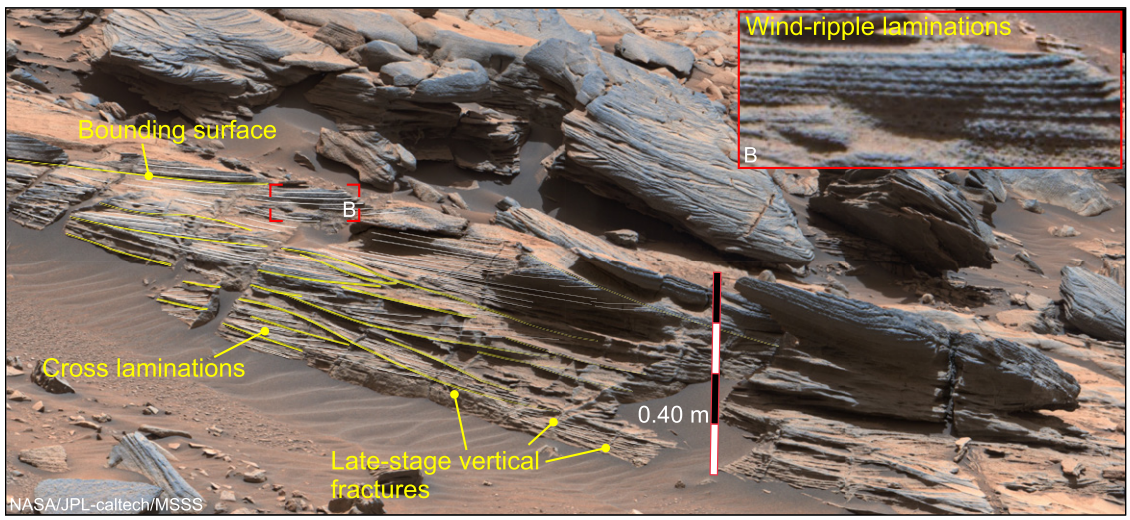


Figure 2. Undeformed strata adjacent to Feòrachas boxwork structure. These sedimentary structures share common characteristics with Stimson formation across plateau. (A) Expression of cross-bedding. (B) Close up of wind-ripple laminations. Credit: NASA/JPL-Caltech/MSSS.

Downloaded from http://pubs.geoscienceworld.org/gsa/geology/article-pdf/52/7/492/6508686/g51849.1.pdf
by guest

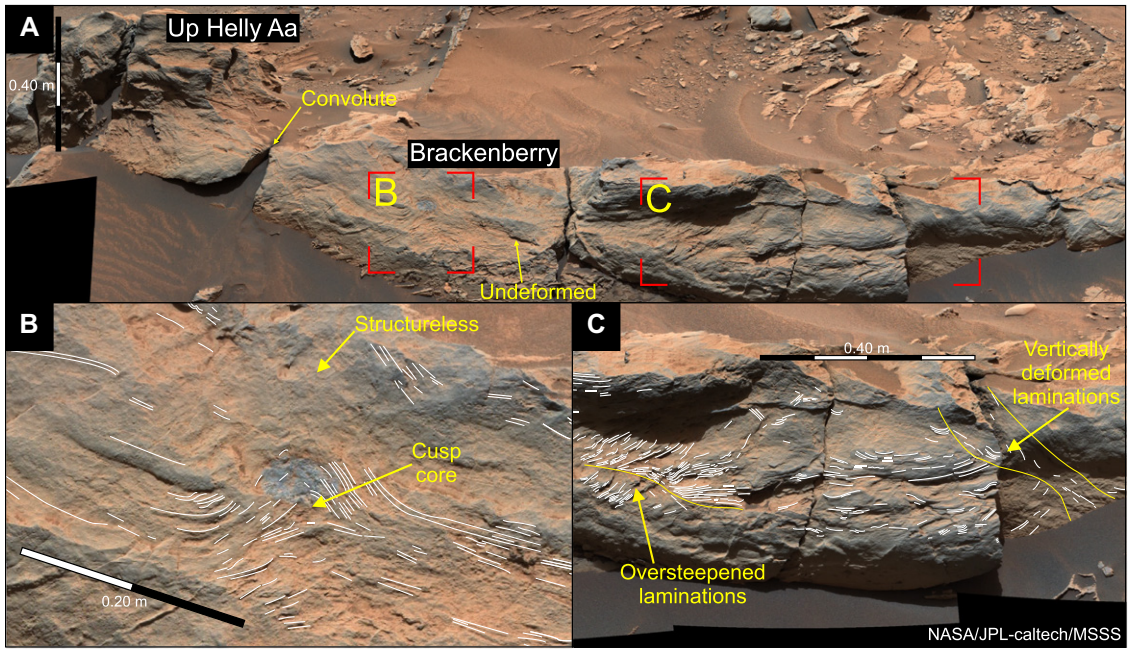


Figure 3. Cusp structures observed at Brackenberry outcrop: (A) context, (B) cusp structure, showing upwarping of laminations and structureless sandstone, and (C) convolute bedding caused by loss of sediment strength. Credit: NASA/JPL-Caltech/MSSS.

laminations (Fig. 2B). Some sets contain subset bounding surfaces (superposition or reactivation surfaces). No interdune deposits are observed. These cross-sets are interpreted as the preserved expression of migrating aeolian dunes in a dry dune field (Banham et al., 2018).

Soft-Sediment Deformation Structures

Soft-sediment deformation structures described as cusps (Owen, 1996) are identified at Brackenberry (Fig. 3A). Figure 3B shows a cusp with laminations in various states of distortion. Toward the core of the cusp, laminations become progressively upwarped, increasing in dip amplitude. Within the center ("cusp core"), an increasing level of deformation is observed, where laminations undulate with increasing amplitude. At the core of the cusp, wind-ripple laminations bend toward vertical, and their coherence is lost; laminations are replaced with largely structureless sandstones in a vertical column several centimeters high. Adjacent to the cusp, laminations are deformed and contorted, forming tight to isoclinal anticlinal folds. Adjacent to this (Fig. 3C), typically planar wind-ripple laminations show complex oversteepening.

Vertically Laminated Structures

Vertically laminated structures are observed at Lamington and Up Helly Aa (Figs. 4A and 4B), and they crosscut the adjacent strata. Up Helly Aa (Fig. 4A) is a resistant sandstone ridge where the ridge adjacent to Brackenberry is cleaved in two by a smaller sandstone dike containing vertical laminations (Figs. 1, 3A, and 4A). On both sides of this dike (Fig. 4B), laminations are deformed and upwarped onto its flanks. At the dike apex, wind-ripple laminations are deformed into a dome structure, forming a cap (Fig. 4B). As the laminations cross over the dike crest, they apparently lose coherence and are difficult to distinguish.

Lamington (Figs. 1 and 4C) is a prominent linear sandstone ridge that runs obliquely to the ridge containing Brackenberry and Up Helly Aa. It is composed of subvertical laminations that are parallel to the dike wall and can be traced along the planform length of the feature (Fig. 4C). In vertical section (Fig. 4D), these laminations are irregular and form groups of radiating subvertical laminations. The margins of the structure are overprinted by erosion-resistant bands that are both vertical and horizontal. These may be later fracture fills that are preferentially cemented. No primary depositional structures can be delineated with certainty.

POSSIBLE MECHANISMS OF DEFORMATION

The formation process of the Feòrachas structure must account for localized deformation of strata, focused in a boxwork pattern; presence of cusp structures deforming primary wind-ripple strata; and vertical laminated ridges. Three plausible modes of formation are presented (which are not mutually exclusive), and each has a common facilitating element: water.

Water-escape mechanisms, driven by lithostatic overburden pressure, could have formed Feòrachas by both liquefaction and fluidization. Where laminations are convoluted and contorted, but show limited shearing, liquefaction is the interpreted deformation mechanism. High fluid pressure could have temporarily overcome overburden pressure, allowing transfer of grain weight to the pore fluid, a loss of sediment strength, and contortion of preexisting sedimentary structures (Lowe, 1975; Owen et al., 2011). The Brackenberry cusp structures (Fig. 3) are interpreted to have formed by fluid shear imparted on unconsolidated sediment grains by water flowing through the pore spaces while escaping vertically to the surface (Owen, 1987). The shearing motion imparted by fluid drag would have formed the upwarped laminations at the fringe of the structure. At the cusp center, where flow through the pore space was greatest, laminations were destroyed, leaving a vertical column of structureless sandstone.

Vertically laminated sandstones at Lamington and Up Helly Aa (Fig. 4) are interpreted to have formed later by sediment injection. These vertical laminations formed in a narrow conduit due to drag forces between the wall and the flow, resulting in accretion of sand onto the walls during a phased emplacement (Peterson, 1968; Whitmore and Strom, 2010; Ross et al., 2014). The position at which the dike reopened may not have been fixed, leading to slight irregularities in thickness and orientation (Fig. 4), contributing to the notion of a phased emplacement, where the central conduit reopened episodically when fluid pressure overcame the overburden pressure (Peterson, 1968). Similar structures are observed in Sacramento Valley (California, USA) (Peterson, 1968) and Antarctica (Taylor, 1982); graded layers of parallel laminations are observed, indicating successive pulses of sediment-bearing fluid injected into a dilating fracture.

The stress regime and mechanical state of the strata controlled the shape and orientation of the structure: Unconsolidated sediments formed pipe structures, as they were unable to support a differential (tensile) stress. To create a dike, the strata must have been partially lithified to have a tensile strength and allow a differential

Downloaded from http://pubs.geoscienceworld.org/gsa/geology/article-pdf/52/7/492/6508686/g51849.1.pdf
by guest

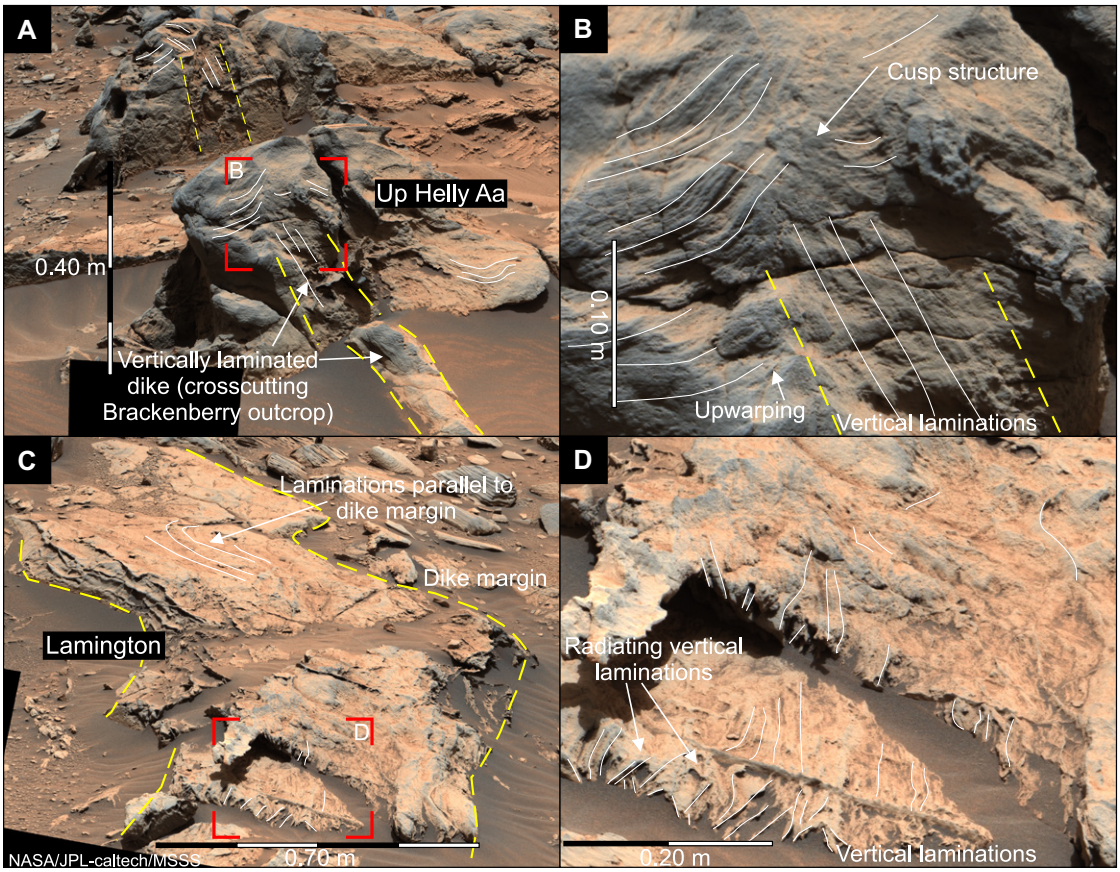


Figure 4. Fluidization structures. (A) Dike structure, with cusp-like structure on apex at Up Helly Aa. (B) Close-up of intersection between dike and cusp structure. (C) Vertically oriented laminations at Lamington. Note: Later fractures crosscut lineament. (D) Close-up showing vertically oriented laminations. Note radiating pattern of vertical laminations. Credit: NASA/JPL-Caltech/MSSS.

horizontal stress to form (Cosgrove, 1995). The orientation of the dikes (215°) indicates tension or extension oriented NW-SE (Fig. 1, rose diagram). This broadly coincides with the slope of the Siccar Point unconformity (Watkins et al., 2022).

Cryogenic processes, such as differential loading by ice, large hydraulic gradients caused by impermeable ice, and freeze-thaw cycling, can all generate conditions where sediment deformation or injection can take place. Water confined by ice can be overpressured and injected into overlying thawed sediment, resulting in clastic dikes. Freeze-thaw cycling can generate sand wedges within the active layer, and polygonal ice wedges form and subsequently melt (or sublime) to leave voids, which are in-filled by windblown sediment. These can have a structureless fill (single event) or be vertically laminated (multiple seasons of freeze-thaw cycles) (Larsen and Mangerud, 1992; Murton et al., 2000). The vertical laminations in the Lamington outcrop could be interpreted as a section through a sand wedge. Infiltration and flow of melt water and freeze-thaw cycles could generate deformation structures and folds like those at Brackenberry. Polygonal sandstone wedges, with deformation of cross-strata attributed to permafrost action, have been identified in Cretaceous aeolian strata in China (Rodríguez-López et al., 2022). While these structures can be explained by processes common to permafrost environments, there is currently no other evidence of glaciation recorded within the Mount Sharp stratigraphy at this time (Grotzinger et al., 2015).

Evaporite-cemented, polygonal, thermal-contraction sandstone wedges can contain vertically laminated sediment bodies within aeolian strata. These form by thermal contraction and expansion of strata weakly bound by evaporites. Structures with similar geometries have been identified in the Page Sandstone (Utah, USA) (Kocurek and Hunter, 1986; Cardenas et al., 2019), forming boxworks with a preferential orientation controlled by the stress regime, coincident with the regional paleodip (Kocurek and Hunter, 1986). The host material requires a tensile strength for fracture formation, in this case provided by an evaporite cement. This commonly forms where the water table is near to the surface, allowing evaporation and precipitation of salt. Modern daily temperature changes of 70 °C are recorded in Gale crater (Vasavada et al., 2017), representing ample conditions for thermal expansion to form fractures. Evaporites are abundant in Gale crater; however, the alpha particle X-ray spectrometer did not identify chemistry consistent with evaporites within the Stimson formation at this location. This does not preclude this mechanism, as evaporites are easily remobilized.

SIGNIFICANCE AND CONCLUSIONS

The presence of water is the common link between the three mechanisms (or combination thereof) proposed to generate the structures seen at Feòrachas. Water would be required at all stages to form the Feòrachas structure: to facilitate binding of the sediment, through cementation or freezing; to create the fractures, by hydrofracturing or frost heave; and finally, to mobilize the sediment, by fluid drag as water moved through the sediment, or through entrainment as water escaped to the surface.

Evidence of water and aqueous sediment transport is abundant within the lower Mount Sharp group strata; however, the stratigraphic sequence records a progressive increase in aridity with increasing elevation. Following the exhumation of Mount Sharp, presumably by wind scouring of fine-grained sediment, which exposed the 5-km-tall central mound, the Stimson formation records accumulation of aeolian strata on the flanks of Mount Sharp in an environment of extreme aridity.

The presence of soft sediment deformation structures, however, provides clear evidence of groundwater penecontemporaneous with the accumulation of the Stimson dune field, as either liquid water or as ice. This evidence for near-surface water in Gale crater during Stimson formation deposition permits interpretations of habitability to extend into younger strata

Downloaded from http://pubs.geoscienceworld.org/gsa/geology/article-pdf/52/7/492/6508686/g51849.1.pdf
by guest

well beyond previously recognized examples within the Mount Sharp group. Moreover, it makes the Stimson or other aeolian strata hosting such structures a viable target in the search for biosignatures.

ACKNOWLEDGMENTS

This research was funded by the U.K. Space Agency, ST/Y000137/1, ST/S001506/1 (S.G. Banham); ST/X002373/1, ST/S001492/1 (S. Gupta); ST/W507520/1 (A. Roberts); and ST/W002566/2 (J. Davis); the Austrian Research Agency, ASAP 892662 Mars-3D (G. Paar); and the National Aeronautics and Space Administration (NASA), 10-MSLPSP10-0012 (D. Rubin). A portion of this research was carried out at the Jet Propulsion Laboratory (JPL), California Institute of Technology, under a contract with NASA (80NM0018D0004) (A. Vasavada and A. Fraeman). This research used data from the NASA Mars Science Laboratory mission. Mastcam mosaics were processed by the Mastcam team at Malin Space Science Systems (credit: NASA/JPL-Caltech/MSSS). Elena Favaro, Ben Cardenas, and anonymous reviewers are thanked for their comments.

REFERENCES CITED

Anderson, R., and Bell, J., 2010, Geologic mapping and characterization of Gale crater and implications for its potential as a Mars Science Laboratory landing site: Mars, v. 5, p. 76–128, https://doi.org/10.1555/mars.2010.0004.

Banham, S.G., et al., 2018, Ancient Martian aeolian processes and palaeomorphology reconstructed from the Stimson formation on the lower slope of Aeolis Mons, Gale crater, Mars: Sedimentology, v. 65, p. 993–1042, https://doi.org/10.1111/sed.12469.

Banham, S.G., et al., 2021, A rock record of complex aeolian bedforms in a Hesperian desert landscape: The Stimson formation as exposed in the Murray buttes, Gale crater, Mars: Journal of Geophysical Research: Planets, v. 126, no. 4, https://doi.org/10.1029/2020JE006554.

Banham, S.G., et al., 2022, Evidence for fluctuating wind in shaping an ancient Martian dune field: The Stimson formation at the Greenheugh pediment, Gale crater: Journal of Geophysical Research: Planets, v. 127, no. 9, https://doi.org/10.1029/2021JE007023.

Bedford, C.C., Schwenzer, S.P., Bridges, J.C., Banham, S., Wiens, R.C., Gasnault, O., Rampe, E.B., Frydenvang, J., and Gasda, P.J., 2020, Geochemical variation in the Stimson formation of Gale crater: Provenance, mineral sorting, and a comparison with modern Martian dunes: Icarus, v. 341, https://doi.org/10.1016/j.icarus.2020.113622.

Bibring, J.-P., et al., 2006, Global mineralogical and aqueous Mars history derived from *OMEGA/Mars Express* data: Science, v. 312, p. 400–404, https://doi.org/10.1126/science.1122659.

Cardenas, B.T., Kocurek, G., Mohrig, D., Swanson, T., Hughes, C.M., and Brothers, S.C., 2019, Preservation of autogenic processes and allogenic forcings in set-scale aeolian architecture II: The scour-and-fill dominated Jurassic Page Sandstone, Arizona, U.S.A.: Journal of Sedimentary Research, v. 89, p. 741–760, https://doi.org/10.2110/jsr.2019.41.

Cosgrove, J.W., 1995, The expression of hydraulic fracturing in rocks and sediments, *in* Ameen, M.S., ed., Fractography: Fracture Topography as a Tool in Fracture Mechanics and Stress Analysis: Geological Society, London, Special Publication 92, p. 187–196, https://doi.org/10.1144/GSL.SP.1995.092.01.10.

Cosgrove, J.W., Banham, S.G., Gupta, S., and Barnes, R., 2022, The origin of the fracture networks in the mudstones of Gale crater, Mars: Their implications regarding the state of stress and fluid pressure during their formation and the depth to which they were buried: Journal of Geophysical Research: Planets, v. 127, no. 12, https://doi.org/10.1029/2022JE007313.

Dietrich, W., Bryk, A., Banham, S., Rubin, D., Thompson, L., Caravaca, G., and Williams, R., 2022, Climate and diagenetic implications of possible soft sediment deformation of the basal aeolian Stimson sediments in Gale crater, *in* 53rd Lunar and Planetary Science Conference, March 2022: The Woodlands, Texas, Lunar and Planetary Institute, https://www.hou.usra.edu/meetings/lpsc2022/pdf/1263.pdf.

Ehlmann, B.L., et al., 2016, The sustainability of habitability on terrestrial planets: Insights, questions, and needed measurements from Mars for understanding the evolution of Earth-like worlds: Journal of Geophysical Research: Planets, v. 121, p. 1927–1961, https://doi.org/10.1002/2016JE005134.

Grotzinger, J.P., et al., 2015, Deposition, exhumation, and paleoclimate of an ancient lake deposit, Gale crater, Mars: Science, v. 350, https://doi.org/10.1126/science.aac7575.

Gwizd, S., et al., 2022, Sedimentological and geochemical perspectives on a marginal lake environment recorded in the Hartmann's Valley and Karasburg members of the Murray formation, Gale crater, Mars: Journal of Geophysical Research: Planets, v. 127, no. 8, https://doi.org/10.1029/2022JE007280.

Kocurek, G., and Hunter, R.E., 1986, Origin of polygonal fractures in sand, uppermost Navajo and Page Sandstones, Page, Arizona: Journal of Sedimentary Petrology, v. 56, p. 895–904, https://doi.org/10.1306/212F8A7B-2B24-11D7-8648000102C1865D.

Kronyak, R.E., Kah, L.C., Miklusicak, N.B., Edgett, K.S., Sun, V.Z., Bryk, A.B., and Williams, R.M.E., 2019, Extensive polygonal fracture network in Siccar Point group strata: Fracture mechanisms and implications for fluid circulation in Gale crater, Mars: Journal of Geophysical Research: Planets, v. 124, p. 2613–2634, https://doi.org/10.1029/2019JE006125.

Larsen, E., and Mangerud, J., 1992, Subglacially formed clastic dikes: Sveriges Geologiska Undersökning, v. 81, p. 163–170.

Lowe, D.R., 1975, Water escape structures in coarse-grained sediments: Sedimentology, v. 22, p. 157–204, https://doi.org/10.1111/j.1365-3091.1975.tb00290.x.

Malin, M.C., et al., 2017, The Mars Science Laboratory (MSL) Mast Cameras and Descent Imager: I. Investigation and instrument descriptions: Earth and Space Science, v. 4, p. 506–539, https://doi.org/10.1002/2016EA000252.

Milliken, R.E., Grotzinger, J.P., and Thomson, B.J., 2010, Paleoclimate of Mars as captured by the stratigraphic record in Gale crater: Geophysical Research Letters, v. 37, L04201, https://doi.org/10.1029/2009GL041870.

Murton, J.B., Worsley, P., and Gozdzik, J., 2000, Sand veins and wedges in cold aeolian environments: Quaternary Science Reviews, v. 19, p. 899–922, https://doi.org/10.1016/S0277-3791(99)00045-1.

Nachon, M., et al., 2014, Calcium sulfate veins characterized by ChemCam/*Curiosity* at Gale crater, Mars: Journal of Geophysical Research: Planets, v. 119, p. 1991–2016, https://doi.org/10.1002/2013JE004588.

Owen, G., 1987, Deformation processes in unconsolidated sands, *in* Jones, M.E., and Preston, R.M.F., eds., Deformation of Sediments and Sedimentary Rocks: Geological Society, London, Special Publication 29, p. 11–24, https://doi.org/10.1144/GSL.SP.1987.029.01.02.

Owen, G., 1996, Anatomy of a water-escape cusp in Upper Proterozoic Torridon Group sandstones, Scotland: Sedimentary Geology, v. 103, p. 117–128, https://doi.org/10.1016/0037-0738(95)00089-5.

Owen, G., Moretti, M., and Alfaro, P., 2011, Recognising triggers for soft-sediment deformation: Current understanding and future directions: Sedimentary Geology, v. 235, p. 133–140, https://doi.org/10.1016/j.sedgeo.2010.12.010.

Peterson, G.L., 1968, Flow structures in sandstone dikes: Sedimentary Geology, v. 2, p. 177–190, https://doi.org/10.1016/0037-0738(68)90024-9.

Rodríguez-López, J.P., Wu, C., Vishnivetskaya, T.A., Murton, J.B., Tang, W., and Ma, C., 2022, Permafrost in the Cretaceous supergreenhouse: Nature Communications, v. 13, 7946, https://doi.org/10.1038/s41467-022-35676-6.

Ross, J.A., Peakall, J., and Keevil, G.M., 2014, Facies and flow regimes of sandstone-hosted columnar intrusions: Insights from the pipes of Kodachrome Basin State Park: Sedimentology, v. 61, p. 1764–1792, https://doi.org/10.1111/sed.12115.

Rubin, D.M., Fairén, A.G., Martínez-Frías, J., Frydenvang, J., Gasnault, O., Gelfenbaum, G., Goetz, W., Grotzinger, J.P., Le Mouélic, S., Mangold, N., Newsom, H., Oehler, D.Z., Rapin, W., Schieber, J., and Wiens, R.C., 2017, Fluidized-sediment pipes in Gale crater, Mars, and possible Earth analogs: Geology, v. 45, p. 7–10, https://doi.org/10.1130/G38339.1.

Taylor, B.J., 1982, Sedimentary dykes, pipes and related structures in the Mesozoic sediments of south-eastern Alexander Island: British Antarctic Survey Bulletin, v. 51, p. 1–42.

Vasavada, A.R., Piqueux, S., Lewis, K.W., Lemmon, M.T., and Smith, M.D., 2017, Thermophysical properties along *Curiosity*'s traverse in Gale crater, Mars, derived from the REMS ground temperature sensor: Icarus, v. 284, p. 372–386, https://doi.org/10.1016/j.icarus.2016.11.035.

Watkins, J.A., Grotzinger, J.P., Stein, N.T., Banham, S.G., Gupta, S., Rubin, D.M., Stack Morgan, K., Edgett, K.S., Frydenvang, J., Siebach, K.L., Lamb, M.P., Sumner, D.Y., and Lewis, K.W., 2022, Burial and exhumation of sedimentary rocks revealed by the base Stimson erosional unconformity, Gale crater, Mars: Journal of Geophysical Research: Planets, v. 127, https://doi.org/10.1029/2022JE007293.

Westall, F., Foucher, F., Bost, N., Bertrand, M., Loizeau, D., Vago, J.L., Kminek, G., Gaboyer, F., Campbell, K.A., Bréhéret, J.-G., Gautret, P., and Cockell, C.S., 2015, Biosignatures on Mars: What, where, and how?: Implications for the search for Martian life: Astrobiology, v. 15, p. 998–1029, https://doi.org/10.1089%2Fast.2015.1374.

Whitmore, J.H., and Strom, R., 2010, Sand injectites at the base of the Coconino Sandstone, Grand Canyon, Arizona (USA): Sedimentary Geology, v. 230, p. 46–59, https://doi.org/10.1016/j.sedgeo.2010.06.022.

Yen, A.S., et al., 2017, Multiple stages of aqueous alteration along fractures in mudstone and sandstone strata in Gale crater, Mars: Earth and Planetary Science Letters, v. 471, p. 186–198, https://doi.org/10.1016/j.epsl.2017.04.033.

Printed in the USA

Downloaded from http://pubs.geoscienceworld.org/gsa/geology/article-pdf/52/7/492/6508686/g51849.1.pdf
by guest